

## Radiative Decay Modes of the Muon\*†

R. R. CRITTENDEN‡ AND W. D. WALKER  
*University of Wisconsin, Madison, Wisconsin*

AND

J. BALLAM§  
*Michigan State University, East Lansing, Michigan*

(Received August 29, 1960)

A 5-in. freon bubble chamber was used to search for the following decay modes of the  $\mu^+$  meson:

- (1)  $\mu^+ \rightarrow e^+ + \gamma$ ,
- (2)  $\mu^+ \rightarrow e^+ + e^- + e^+$ ,
- (3)  $\mu^+ \rightarrow e^+ + \nu^0 + \bar{\nu}^0 + \gamma$ ,
- (4)  $\mu^+ \rightarrow e^+ + \nu^0 + \bar{\nu}^0 + e^+ + e^-$ .

Two exposures were made at the Carnegie Institute of Technology synchrocyclotron. A total of 200 000 pictures were taken yielding  $3.3 \times 10^5$   $\mu^+$  meson decays.

A total of  $3 \times 10^5$   $\mu^+$  decays were examined for mode (1). No decays consistent with this mode were found. The upper limit on the branching ratio  $R_{\text{rad}}$  was found to be

$$R_{\text{rad}} = (\mu^+ \rightarrow e^+ + \gamma) / (\mu^+ \rightarrow e^+ + \nu^0 + \bar{\nu}^0) < 2.5 \times 10^{-5}.$$

A total of  $3.3 \times 10^5$   $\mu^+$  decays were scanned for mode (2) and no such decays were observed. The limit on the branching ratio  $R_{3e}$  was found to be

$$R_{3e} = (\mu^+ \rightarrow e^+ + e^- + e^+) / (\mu^+ \rightarrow e^+ + \nu^0 + \bar{\nu}^0) < 4 \times 10^{-6}.$$

The internal bremsstrahlung rate (mode 3) was measured for two values of  $E_{\gamma 0}$  (the minimum photon energy detected). The results were

$$\begin{aligned} R_{\text{IB}} &= (\mu^+ \rightarrow e^+ + \nu^0 + \bar{\nu}^0 + \gamma) / (\mu^+ \rightarrow e^+ + \nu^0 + \bar{\nu}^0), \\ R_{\text{IB}} &= (1.4 \pm 0.4) \times 10^{-2}, \quad E_{\gamma 0} = 10 \text{ Mev}, \\ R_{\text{IB}} &= (3.3 \pm 1.3) \times 10^{-3}, \quad E_{\gamma 0} = 20 \text{ Mev}. \end{aligned}$$

The rate of internal conversion of internal bremsstrahlung [mode (4)] was found to be

$$R_{\text{IC}} = (\mu^+ \rightarrow e^+ + \nu^0 + \bar{\nu}^0 + e^+ + e^-) / (\mu^+ \rightarrow e^+ + \nu^0 + \bar{\nu}^0) = (2.2 \pm 1.5) \times 10^{-5}, \quad E_0 = 10 \text{ Mev},$$

where  $E_0$  is the minimum energy of the internally converted  $\gamma$  ray.

A summary is given of previous experiments on these decay modes and results are discussed with special reference to the intermediate boson scheme of weak four-fermion interactions.

## I. INTRODUCTION

A. Intermediate Bosons and  $\mu^+ \rightarrow e^+ + \gamma$ 

It has been suggested<sup>1</sup> that the muon decay may take place through an intermediate boson which is coupled weakly to the lepton fields. If the intermediate boson is taken to be a charged spin-one boson, then it can be used to explain the  $V-A$  form of weak decay interactions.<sup>2</sup> Such a theory would require that diagrams of the form of Fig. 1(a), where  $f_1, f_2, f_3, f_4$  are fermions, be replaced by diagrams of the form of Fig. 1(b), where  $W$  is the intermediate boson. If  $W$  has no

neutral state, then decays involving neutral currents such as

$$\begin{aligned} \mu^\pm &\rightarrow e^\pm + e^- + e^+, \\ K^\pm &\rightarrow \pi^\pm + e^- + e^+, \\ K^\pm &\rightarrow \pi^\pm + \mu^+ + \mu^-, \end{aligned}$$

will be forbidden. If muon decay does take place through an intermediate charged vector boson, then the decay mode  $\mu^+ \rightarrow e^+ + \gamma$  might be expected to occur. Using the assumptions of a charged intermediate vector boson, the two-component neutrino, and lepton conservation, the branching ratio

$$R_{\text{rad}} = (\mu^+ \rightarrow e^+ + \gamma) / (\mu^+ \rightarrow e^+ + \nu^0 + \bar{\nu}^0)$$

has been calculated by several people.<sup>3</sup> The result is ambiguous, however, since it depends upon the mass and magnetic moment of the vector boson. If the mass of the boson is taken to be approximately that of the  $K$  meson or if the anomalous magnetic moment of the

\* Supported in part by the U. S. Atomic Energy Commission and in part by the Research Committee of the University of Wisconsin with funds provided by the Wisconsin Alumni Research Foundation.

† This work has been submitted by R. R. Crittenden to the University of Wisconsin in partial fulfillment of the requirements for the degree of Doctor of Philosophy.

‡ Present address: Brookhaven National Laboratory, Upton, New York.

§ Supported in part by the National Science Foundation.

<sup>1</sup> H. Yukawa, *Revs. Modern Phys.* **21**, 474 (1949).

<sup>2</sup> R. P. Feynman and M. Gell-Mann, *Phys. Rev.* **109**, 193 (1958); J. Schwinger, *Ann. Phys.* **2**, 407 (1957).

<sup>3</sup> G. Feinberg, *Phys. Rev.* **110**, 1482 (1958); M. Ebel and F. Ernst (to be published); P. Meyer and G. Salzman (to be published).

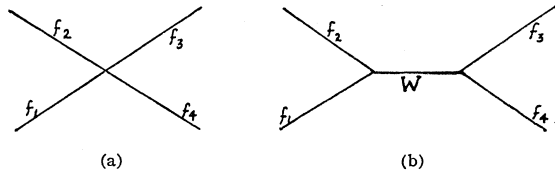


FIG. 1. Feynman diagrams for the four-fermion interaction.

boson is taken to be 1, then one obtains a branching ratio  $R_{\text{rad}} \approx 8 \times 10^{-4}$ . However, for other values of mass and magnetic moment the branching ratio may be small. In particular Ebel and Ernst have shown that for an anomalous moment of 0.7 the branching ratio would be less than  $10^{-6}$  for a wide variation of masses.

The calculation of  $R_{\text{rad}}$  has also been made under the assumption of a charged scalar intermediate boson.<sup>4</sup> This gives

$$R_{\text{rad}} \approx \alpha / 24\pi \\ \approx 10^{-4}.$$

This result, unlike that for the vector boson, is both convergent and unambiguous. It is also very much in disagreement with experimental results. One may forbid both  $\mu^\pm \rightarrow e^\pm + e^- + e^+$  and  $\mu^\pm \rightarrow e^\pm + \gamma$  by retaining the intermediate boson and assigning different lepton numbers to  $\mu^+$  and  $e^+$ .<sup>5</sup> This requires a 4-component neutrino theory to give the correct  $\mu$ -decay spectrum.

### B. Previous Experiments

A number of experiments have been carried out in an attempt to detect  $\mu^+ \rightarrow e^+ + \gamma$  and  $\mu^+ \rightarrow e^+ + e^- + e^+$ . Table I gives a summary of the experiments on  $\mu^+ \rightarrow$

TABLE I. Summary of experimental results for the branching ratio  $R_{\text{rad}} = (\mu^+ \rightarrow e^+ + \gamma) / (\mu^+ \rightarrow e^+ + \nu^0 + \bar{\nu}^0)$ .

Reference	Technique	$R_{\text{rad}}$
Lokanathan and Steinberger <sup>a</sup>	Electronics	$< 2 \times 10^{-5}$
Davis, Roberts, and Zipf <sup>b</sup>	Electronics	$< 1 \times 10^{-5}$
Berley, Lee, and Bardon <sup>c</sup>	Electronics	$< 2 \times 10^{-6}$
O'Keefe <sup>d</sup>	Electronics	$< 2 \times 10^{-6}$
Krestnikov <sup>e</sup>	Freon bubble chamber	$< 4 \times 10^{-5}$
Ashkin, Fazzini, Fidecaro, Lipman, Merrison, and Paul <sup>f</sup>	Electronics	$< 1.3 \times 10^{-6}$
Frankel, Hagopian, Halpern, and Whetstone <sup>g</sup>	Electronics	$< 1.2 \times 10^{-6}$

<sup>a</sup> S. Lokanathan and J. Steinberger, Phys. Rev. **98**, 240(A) (1955).

<sup>b</sup> H. F. Davis, A. Roberts, and T. F. Zipf, Phys. Rev. Letters **2**, 211 (1959).

<sup>c</sup> D. Berley, J. Lee, and M. Bardon, Phys. Rev. Letters **2**, 357 (1959).

<sup>d</sup> T. O'Keefe, M. Rigby, and J. Wormald, Proc. Phys. Soc. (London) **73**, 951 (1959).

<sup>e</sup> Y. Krestnikov, Ninth Annual International Conference on High-Energy Physics, Kiev, 1959 (unpublished).

<sup>f</sup> J. Ashkin, T. Fazzini, G. Fidecaro, N. H. Lipman, A. W. Merrison, and H. Paul (to be published).

<sup>g</sup> S. Frankel, V. Hagopian, J. Halpern, and A. L. Whetstone, Phys. Rev. **118**, 589 (1960).

<sup>4</sup> C. Fronsald and S. L. Glashow, Phys. Rev. Letters **3**, 570 (1959).

<sup>5</sup> E. J. Mahmoud and H. M. Konopinski, Phys. Rev. **92**, 1045 (1953); J. Schwinger, Ann. Phys. **2**, 407 (1957).

TABLE II. Summary of experimental results for the branching ratio  $R_{3e} = (\mu^+ \rightarrow e^+ + e^- + e^+) / (\mu^+ \rightarrow e^+ + \nu^0 + \bar{\nu}^0)$ .

Reference	Technique	$R_{\text{rad}}$
Lee and Samios <sup>a</sup>	H <sub>2</sub> bubble chamber	$< 1 \times 10^{-5}$
Gurevich <sup>b</sup>	Emulsion	$< 2 \times 10^{-5}$
Krestnikov <sup>c</sup>	Freon bubble chamber	$< 1 \times 10^{-5}$

<sup>a</sup> J. Lee and N. P. Samios, Phys. Rev. Letters **3**, 55 (1959).

<sup>b</sup> I. Gurevich *et al.*, Ninth Annual International Conference on High-Energy Physics, Kiev, 1959 (unpublished).

<sup>c</sup> Y. Krestnikov, see footnote b.

$e^+ + \gamma$  and Table II summarizes the experiments on  $\mu^+ \rightarrow e^+ + e^- + e^+$ .

### C. Intermediate Boson and $\mu^+ \rightarrow e^+ + \nu^0 + \bar{\nu}^0 + \gamma$ Decay

Another method of detecting the existence of an intermediate boson in the muon decay process has been proposed by Eckstein and Pratt.<sup>6</sup> They examine the effect of such a meson on the internal bremsstrahlung process. The branching ratio  $R_{\text{IB}} = (\mu^+ \rightarrow e^+ + \nu^0 + \bar{\nu}^0 + \gamma) / (\mu^+ \rightarrow e^+ + \nu^0 + \bar{\nu}^0)$  for this process is of course infrared divergent and therefore depends upon the lower limit of the energy of the detected  $\gamma$  rays. Several authors<sup>7</sup> have made the calculation for  $R_{\text{IB}}$  assuming no intermediate boson. The branching ratio was found to be

$$R_{\text{IB}} = \frac{\alpha}{3\pi} \left\{ \left( \ln \frac{M_\mu}{M_e} - \frac{17}{12} \right) \left[ 6 \ln \frac{1}{y_0} - 6(1-y_0) - (1-y_0)^4 \right] \right. \\ \left. + 3[L(1) - L(y_0)] - \frac{1}{2}[6 + (1-y_0)^2](1-y_0) \ln(1-y_0) \right. \\ \left. + \frac{1}{48}(1-y_0)(125 + 45y_0 - 33y_0^2 + 7y_0^3) \right\},$$

where<sup>8</sup>

$$L(x) = \int_0^x t^{-1} \ln |1-t| dt, \quad y_0 = 2E_0/M_\mu.$$

$E_0$  is the minimum photon energy,  $M_\mu$  is the mass of the muon, and  $M_e$  is the electron mass. For  $E_0 = 10$  Mev this gives  $R_{\text{IB}} = 1.3 \times 10^{-2}$  and for  $E_0 = 20$  Mev,  $R_{\text{IB}} = 4.4 \times 10^{-3}$ . The spectral distribution of photons is

$$\frac{dN}{dy} = N_\mu \frac{\alpha}{3\pi} (1-y) \left\{ \left[ 2 \ln \frac{M_\mu}{M_e} - \frac{17}{6} + \ln(1-y) \right] \right. \\ \left. \times \left[ \frac{3}{y} - 2(1-y)^2 - \frac{1}{12}(1-y)(22-13y) \right] \right\}.$$

Pratt and Eckstein found that on the basis of the intermediate charged vector boson theory the branching

<sup>6</sup> S. G. Eckstein and R. H. Pratt, Ann. Phys. (to be published).

<sup>7</sup> T. Kinoshita and A. Sirlin, Phys. Rev. Letters **2**, 177 (1959); S. G. Eckstein and R. H. Pratt, Ann. Phys. (to be published); C. Fronsald and H. Überall, Phys. Rev. **113**, 654 (1959).

<sup>8</sup> For a tabulation of this function see K. Mitchell, Phil. Mag. **40**, 351 (1949).

ratio contains additional terms with coefficients in powers of  $M_\mu/M_e$ . They considered the first order term and found that for an intermediate boson with mass about equal to that of the  $K$  meson the branching ratio  $R_{IB}$  is changed by a few percent. This of course is a very small effect to be detected by present experimental techniques. It is of interest, however, since it is independent of whether the neutrino associated with the muon is the same as the neutrino associated with the electron.

The method of Kroll and Wada<sup>9</sup> was used by Pratt and Eckstein to find also the branching ratio

$$R_{IC} = (\mu^+ \rightarrow e^+ + \nu^0 + \bar{\nu}^0 + e^+ + e^-) / (\mu^+ \rightarrow e^+ + \nu^0 + \bar{\nu}^0).$$

The result depends upon the lower limit  $E_0$  of the total energy of the internally converted photon. For  $E_0 = 10$  Mev they found  $R_{IC} \sim 4 \times 10^{-5}$ .

## II. PROCEDURE

### A. Exposures

The 5-in. freon ( $\text{CF}_3\text{Br}$ ) bubble chamber, which is described by Crittenden<sup>10</sup> was used to search for the following decay modes of the muon:

- (1)  $\mu^+ \rightarrow e^+ + \gamma$ ,
- (2)  $\mu^+ \rightarrow e^+ + e^- + e^+$ ,
- (3)  $\mu^+ \rightarrow e^+ + \nu^0 + \bar{\nu}^0 + \gamma$ ,
- (4)  $\mu^+ \rightarrow e^+ + \nu^0 + \bar{\nu}^0 + e^+ + e^-$ .

Two exposures were made with this chamber at the Carnegie Institute of Technology synchrocyclotron. The first of these was made in August, 1958 and yielded a total of 60 000 pictures. The second exposure was made in February, 1959 and produced 140 000 pictures. The chamber was operated at  $48^\circ\text{C}$  at a repetition rate of one expansion per second. The  $\pi^+$  mesons produced by the internal proton beam were analyzed by passing them through a bending magnet. The resulting beam was moderated by copper absorber until the pions were stopped near the center of the chamber. These  $\pi^+$  mesons then served as a source of  $\mu^+$  mesons. The range in freon of the muon from  $\pi^+ \rightarrow \mu^+ + \nu^0$  is about 1 mm.

Figure 2 is a schematic drawing of the experimental arrangement.

### B. Scanning

The stereo views of the chamber were photographed adjacently on the same film. Both views were projected adjacently at a magnification of twice life size and scanning was carried out on the two views at the same time. The film was first scanned for all interesting events and the frame number of such events was

<sup>9</sup> N. Kroll and W. W. Wada, Phys. Rev. **98**, 1355 (1955).

<sup>10</sup> R. R. Crittenden, Ph.D. thesis, University of Wisconsin, 1960 (unpublished).

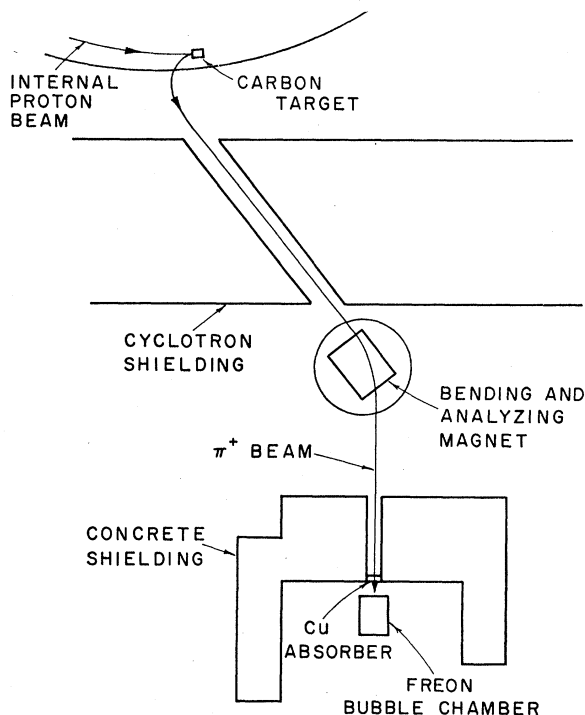


FIG. 2. The experimental arrangement at the Carnegie Institute of Technology synchrocyclotron.

recorded. At a later time the pictures were reprojected and measurements of projected angles and coordinates were made. These data were then punched in IBM cards. An IBM 650 was programmed to reconstruct the events in bubble chamber space. Details of the geometry are given in reference 10. The running time on the IBM 650 for one event was about  $2\frac{1}{2}$  seconds.

All events which survived the scanning criteria (described in III) were then re-examined. Multiple scattering measurements were made on the pair electrons and estimates were made of their total range. Both of these methods of energy measurements are, of course, quite crude for electrons because of the high probability for large energy losses to a single photon through bremsstrahlung. The critical energy  $E_c$  (the energy at which the rates of energy loss by radiation and ionization are equal) is given by<sup>11</sup>

$$E_c = 1600 M_e c^2 / Z,$$

where  $M_e$  is the mass of the electron and  $Z$  is the charge number of the absorber. For freon ( $\text{CF}_3\text{Br}$ ),  $E_c$  is about 60 Mev. The ratio of radiative loss to collision loss is

$$\frac{(dE/dx)_{\text{rad}}}{(dE/dx)_{\text{coll}}} \sim \frac{E_0 Z}{1600 M_e c^2}.$$

Thus the rate of energy loss by a 5-Mev electron in

<sup>11</sup> H. A. Bethe and W. Heitler, Proc. Roy. Soc. (London) **A146**, 83 (1934).

freon due to radiation is about 7% of the rate due to ionization. At 10 Mev the radiation loss rate is about 13% of the ionization loss rate. Therefore, it should be possible to make use of multiple scattering and range in establishing a lower limit for the energies of electron pairs providing the limit is well below  $E_c$ .

Multiple scattering measurements were made using a modified microscope stage in conjunction with the regular scanning projector. The cell size was chosen to give a signal to noise ratio of 2 at an electron energy of 15 Mev. The noise was determined by means of measurements on 25 of the cosmic rays which passed through the chamber during the course of the experiment. This resulted in the use of 3-mm cells on the projected image which corresponds to approximately 1.5 mm in real space. The constant cell size method was used instead of the constant-sagitta method, because the primary objective was the establishment of a lower energy limit and not the actual determination of energies.

The root-mean-square second differences were then used to solve for  $p\beta$  in the equation

$$\langle D_s^2 \rangle^{\frac{1}{2}} = E_s X^{\frac{1}{2}} / p\beta L_0^{\frac{1}{2}},$$

where  $X$  is the cell size (3 mm),  $L_0$  is the radiation length (25 cm in projection space) and  $E_s$  is a constant (21 Mev).

Multiple scattering was attempted only on those tracks for which it was possible to obtain 6 or more second differences.

A comparison of the multiple scattering and range measurements is shown in Fig. 3. A point on this plot represents an electron whose energy as determined by multiple scattering is given by the abscissa and whose energy as obtained by range is given by the ordinate. The points should of course fall along a straight line, which has a slope of one and which passes through the origin, if the two methods are accurate. Because of the

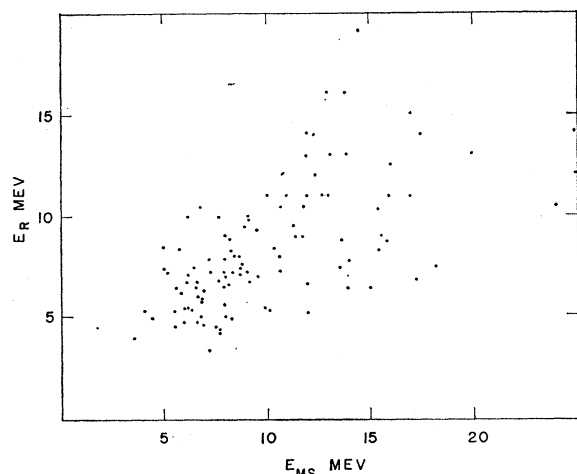


FIG. 3. The correlation between the energies of 107 electrons as measured by multiple scattering,  $E_{MS}$ , and range,  $E_R$ .

effects of bremsstrahlung, the multiple scattering measurements should be more accurate than range measurements at higher energies, with range measurements giving an energy which is too low. The plot is in qualitative agreement with this. When it was possible, both methods were used to determine the energy of an electron and the results were averaged with equal weights.

### III. RESULTS

#### A. $\mu^+ \rightarrow e^+ + \gamma$

Since the muons decayed at rest and this is a two-body decay process, a muon decaying by this mode would produce an electron and a  $\gamma$  ray of equal and opposite momenta and total energy equal to the rest mass of the muon. The pictures were therefore scanned for high-energy pairs which appeared to originate from a muon ending and which made an angle of  $180^\circ$  with respect to a high-energy decay electron.

The possible sources of background for this decay mode were the following:

(1) A flux of  $\gamma$  rays in the beam direction which originated in the absorber or in the beam port. Since these  $\gamma$  rays had momenta roughly parallel to the axis of symmetry of the stereo system, discrimination against them was difficult. For this reason only those events in which both the decay electron and the  $\gamma$  ray made an angle of more than  $10^\circ$  to the front and back beam direction were accepted. This resulted in a ten percent loss in counting rate, but virtually eliminated all the random background pairs for this process.

(2) High-energy  $\gamma$  rays emitted in the backward direction, i.e., opposite the electron, from  $\mu^+ \rightarrow e^+ + \nu^0 + \bar{\nu}^0 + \gamma$ . Both theoretical results<sup>12</sup> and experimental data on  $\mu^+ \rightarrow e^+ + \nu^0 + \bar{\nu}^0 + \gamma$  indicated that this source of background was negligible in this experiment.

A total of  $3 \times 10^5$   $\mu^+$  endings were scanned for the  $\mu^+ \rightarrow e^+ + \gamma$  decay mode. No decays consistent with  $\mu^+ \rightarrow e^+ + \gamma$  were found.

In order to estimate the detection efficiency, it is necessary to know what was the mean path available to a  $\gamma$  ray for conversion into an electron pair. The illuminated volume of the chamber was essentially that of a cylinder of radius  $R_0$  and height  $H$ . Let us assume that the  $\mu^+$  decayed at the center of this volume. The mean radius will then be given by

$$4\pi\langle r \rangle = 2 \int_{\tan^{-1}(H/2R_0)}^{\pi/2} \left[ \frac{R_0}{\sin\theta} - 2\pi \sin\theta \right] d\theta + 2 \int_0^{\tan^{-1}(H/2R_0)} \left[ \frac{H}{2 \cos\theta} - 2\pi \sin\theta \right] d\theta,$$

or

$$\langle r \rangle = \frac{\pi}{2} R_0 + \frac{H}{2} \ln \left( \frac{4R_0^2 + H^2}{4R_0^2} \right) - R \tan^{-1} \frac{H}{2R_0}.$$

<sup>12</sup> C. FronsdaI and H. Überall, Phys. Rev. **113**, 654 (1959).

This result is approximately correct even if the decay point is not at the center. For the bubble chamber used in this experiment  $R=5$  cm and  $H=9$  cm. However, in order for a pair to be identified it must be formed at least 1.5 cm from the wall. Therefore, for the purpose of this calculation  $H=6$  cm,  $R=3.5$  cm. Thus  $\langle r \rangle = 4.6$  cm.

The probability for pair production by a 50-Mev  $\gamma$  ray is 0.43 per radiation length  $L_0$ . The radiation length is given by<sup>11</sup>

$$L_0 = [4\alpha(N/A)Z(Z+1)r_e \ln(183/Z^{1/2})]^{-1},$$

where  $\alpha$  is the fine structure constant,  $N$  is Avogadro's number,  $A$  is the atomic weight of the absorber,  $Z$  is the atomic number of the absorber, and  $r_e$  is the classical radius of the electron. For  $\text{CF}_3\text{Br}$  this gives  $L_0=12.5$  cm. Thus the probability for producing a visible pair was  $P=(0.43)(4.6/12.5)=0.16$ . The scanning efficiency was estimated on the basis of results on  $\mu^+ \rightarrow e^+ + \nu^0 + \bar{\nu}^0 + \gamma$  to be about 85%. Therefore, the total detection efficiency for  $\mu^+ \rightarrow e^+ + \gamma$  was 13.5%. Thus it was found that

$$R_{\text{rad}} < 1/(0.135)(3 \times 10^5), \quad R_{\text{rad}} < 2.5 \times 10^{-5},$$

### B. $\mu^+ \rightarrow e^+ + e^- + e^+$

A total of  $3.3 \times 10^5$   $\mu^+$  decays were scanned for the three-electron decay mode. The principal test for this mode was momentum balance. Since it is a decay into three visible charged particles from a particle at rest, it would have to produce three coplanar electrons whose total energy was 106 Mev.

The background for this process came from the following:

(1) The decay mode  $\mu^+ \rightarrow e^+ + \nu^0 + \bar{\nu}^0 + e^+ + e^-$ . In this case the electrons would in general be noncoplanar and would have a total energy of less than 106 Mev.

(2)  $\mu^+ \rightarrow e^+ + \nu^0 + \bar{\nu}^0 + \gamma$  where pair production by the  $\gamma$  ray took place near the  $\mu^+$  ending. The same arguments apply here as in (1).

(3) A  $\gamma$  ray entering with the beam or coming from the walls of the chamber and accidentally producing a pair near a  $\mu^+$  ending. The density  $\rho_p$  of pairs per  $\mu^+$  per  $\text{cm}^3$  was  $4.5 \times 10^{-4} (1/\mu^+ \text{ cm}^3)$ . In order to be confused with  $\mu^+ \rightarrow 2e^+ + e^-$  the vertex of the pair would have to be within a radius of about 1.5 mm of the  $\mu^+$  decay point. Thus the number of such accidents would be given by

$$\begin{aligned} N &= \frac{4}{3}\pi r^3 \rho_p N_\mu \\ &= \frac{4}{3}\pi (0.15)^3 (4.5 \times 10^{-4}) N_\mu \\ &= 6.4 \times 10^{-6} N_\mu. \end{aligned}$$

This of course is only an upper limit since in addition the accident would have to occur in such a way as to indicate momentum and energy conservation.

No examples were found of  $\mu^+$  decays consistent with  $\mu^+ \rightarrow e^+ + e^- + e^+$  in a total of  $3 \times 10^6$  stopped  $\mu^+$ . The

scanning efficiency was estimated to be at least 85%. Thus the upper limit on the branching ratio

$$R_{3e} = (\mu^+ \rightarrow e^+ + e^- + e^+) / (\mu^+ \rightarrow e^+ + \nu^0 + \bar{\nu}^0)$$

was found to be

$$R_{3e} < 1/(0.85)(3.3 \times 10^5), \quad R_{3e} < 4 \times 10^{-6}.$$

### C. $\mu^+ \rightarrow e^+ + \nu^0 + \bar{\nu}^0 + \gamma$

The  $\gamma$  rays from this decay mode have a continuous spectrum of energies from 0 to 52 Mev. Just as in the case of ordinary bremsstrahlung, the most probable angle of emission is near zero degrees.<sup>12</sup>

The background for this mode of decay came from the following sources:

(1) Random  $\gamma$  rays which entered with the beam or were produced in the walls of the chamber and accidentally correlated with a  $\mu^+$  ending. As mentioned above the flux of  $\gamma$  rays in the beam direction was quite high and since the line of symmetry for the stereo cameras was also in that direction, discrimination against this background was difficult. For these reasons only those events in which both the decay electron and the correlated pair made a projected angle of more than  $30^\circ$  with respect to the front and back beam direction were accepted. This resulted in a 36% loss of counting rate, but eliminated virtually all of the background from this source. The remaining random background was estimated as follows: Let the mean density of  $\mu^+$  endings per unit volume per picture be  $\rho_\mu$ , the total number random pairs per  $\mu^+$  be  $N_p$ , the opening angle between electrons in a pair be  $\varphi$ , the distance from a  $\mu^+$  ending to a correlated pair vertex be  $R$ , and the number of  $\mu^+$ 's be  $N_\mu$ . Then

$$dN_{pc}/dR = \pi \rho_\mu N_p R^2 \varphi^2 N_\mu.$$

Experimentally it was found that  $\rho_\mu = 4.5 \times 10^{-3} \mu^+/\text{cm}^3$ ,

$$N_p = 0.1 (1/\mu^+), \quad \varphi = 0.1 \text{ rad.}$$

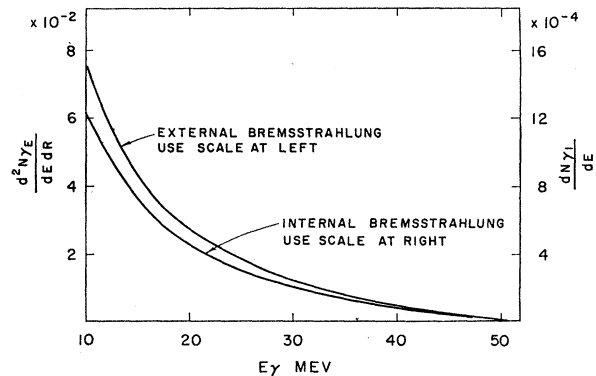


FIG. 4. The spectral distribution of  $\gamma$  rays from external and internal bremsstrahlung. The quantity  $d^2N_{\gamma p}/dE dR$  is the differential probability per radiation length, per Mev that a photon of energy  $E$  will be produced by bremsstrahlung of a  $\mu$ -decay electron and  $dN_{\gamma 1}/dE$  is the differential probability per Mev that a photon of energy  $E$  will be produced by  $\mu^+ \rightarrow e^+ + \nu^0 + \bar{\nu}^0 + \gamma$ .

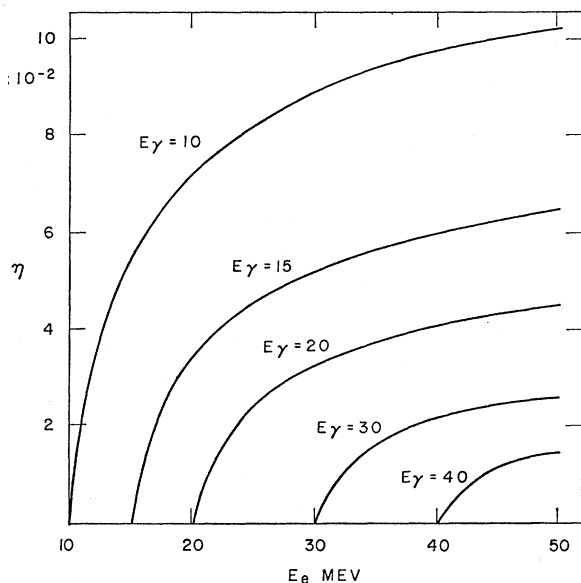


FIG. 5. The differential probability  $\eta(E, E')$  per radiation length, per Mev that an electron of energy  $E'$  will produce a photon of energy  $E$  [B. Rossi, *High-Energy Particles* (Prentice Hall, Inc., Englewood Cliffs, New Jersey, 1952), Chap. 2].

This gives

$$dN_{pc}/dR = 1.4 \times 10^{-5} N_{\mu} R^2.$$

For small values of  $R$  this background was small compared to internal and external bremsstrahlung.

(2) External bremsstrahlung by normal  $\mu^+$ -decay electrons.

From Fig. 4 it can be seen that the spectral distributions of  $\gamma$  rays from the internal and external bremsstrahlung processes are approximately of the same form. The angular dependence is also very similar. The spatial distribution of pairs formed from the two bremsstrahlung processes is different, however. If we let  $N_{\gamma I}$  be the number of  $\gamma$  rays from internal bremsstrahlung,  $N_{\gamma E}$  be the number of  $\gamma$  rays from external bremsstrahlung,  $N_{\gamma T}$  be the total number of  $\gamma$  rays from both internal and external bremsstrahlung,  $N_e$  be the number of electrons from  $\mu^+$  decay,  $R$  be the distance from a  $\mu^+$  ending to an electron pair vertex,  $\lambda_b$  be the mean distance for bremsstrahlung of an electron and  $\lambda_p$  be the mean distance for pair production by a  $\gamma$  ray, then

$$\begin{aligned} \frac{dN_{\gamma T}}{dR} &= \frac{dN_{\gamma E}}{dR} + \frac{dN_{\gamma I}}{dR} \\ &= -\frac{1}{\lambda_b} N_e - \frac{1}{\lambda_p} N_{\gamma E} - \frac{1}{\lambda_p} N_{\gamma I}, \end{aligned}$$

or

$$N_{\gamma T} = \frac{N_e(0)(1/\lambda_b)}{1/\lambda_b - 1/\lambda_p} [e^{-R/\lambda_p} - e^{-R/\lambda_b}] + N_{\gamma I}(0)e^{-R/\lambda_p}.$$

If  $R \ll \lambda_b \approx \lambda_p$ , then

$$N_{\gamma T} = (1/\lambda_b)N_e(0)R + N_{\gamma I}(0).$$

The total number of pairs  $N_{pT}$  originating in an interval  $dR$  at  $R$  will then be

$$\frac{dN_{pT}}{dR} = \frac{1}{\lambda_p \lambda_b} N_e(0)R + \frac{1}{\lambda_p} N_{\gamma I}(0).$$

At the energies concerned, both  $\lambda_b$  and  $\lambda_p$  are energy dependent. Furthermore, a pair will not be recognized as such unless both the electron and positron have energy greater than some minimum value, say enough to produce five bubbles. This effect of energy sharing is energy dependent also. This may be expressed by writing

$$\lambda_b = L_0/\eta(E, E'), \quad \lambda_p = L_0/\varphi(E, E_m),$$

where  $L_0$  is the radiation length,  $\eta(E, E')$  is the probability per radiation length that an electron of energy  $E'$  will produce a photon of energy  $E$  and  $\varphi(E, E_m)$  is the probability per radiation length that a photon of energy  $E$  will produce a pair in which both the electron and the positron have energies greater than  $E_m$ . The functions  $\eta$  and  $\varphi$  are shown in Fig. 5 and Fig. 6.

The energy spectrum of electrons from normal  $\mu$  decay is<sup>13</sup>

$$dN_e/dE = 16E^2/M_{\mu}^4(3M_{\mu} - 4E).$$

The spectral distribution of  $\gamma$  rays from  $\mu^+ \rightarrow e^+ + \nu^0 + \bar{\nu}^0 + \gamma$  as given by Kinoshita and Sirlin<sup>7</sup> is given in Sec. I.

The total number of pairs originating in  $dR$  at  $R$  with total energy greater than  $E_0$  and with both electron

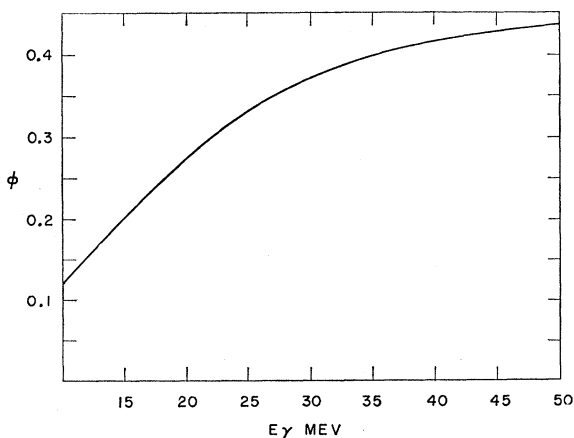


FIG. 6. The differential probability  $\varphi(E, E_m)$  per radiation length, per Mev that a photon of energy  $E$  will produce an electron pair in which both electrons have energy greater than  $E_m$  (Rossi, see Fig. 5 caption). In this case  $E_m = 2$  Mev.

<sup>13</sup> Assuming the Michel parameter [L. Michel, Proc. Phys. Soc. (London) A63, 514 and 1371 (1950)] to be equal to  $\frac{3}{4}$ .

and positron having energy greater than  $E_m$  is then

$$\frac{dN_{pT}}{dR} = \int_{E_0}^{M_{\mu/2}} \frac{\varphi(E, E_m)}{L_0} \left[ \frac{dN_{\gamma I}(E)}{dE} + R \int_E^{M_{\mu/2}} \frac{dN_e(E')}{dE'} \frac{\eta(E', E)}{L_0} dE' \right] dE.$$

The spectral distribution of pairs from internal and external bremsstrahlung, i.e.,

$$\frac{\varphi(E, E_m)}{L_0} \frac{dN_{\gamma I}(E)}{dE}$$

and

$$\frac{\varphi(E, E_m)}{L_0} \int_E^{M_{\mu/2}} \frac{dN_e(E')}{dE'} \frac{\eta(E', E)}{L_0} dE',$$

are shown in Fig. 7.

The integration was done numerically and gave the following:

$$\left. \begin{array}{l} E_0 = 10 \text{ Mev} \\ E_m = 2 \text{ Mev} \end{array} \right\} \frac{dN_{pT}}{dR} = 2.5 \times 10^{-4} \frac{1}{\mu^+ \text{ cm}} + 12 \times 10^{-4} \frac{R}{\mu^+ \text{ cm}^2},$$

$$\left. \begin{array}{l} E_0 = 20 \text{ Mev} \\ E_m = 2 \text{ Mev} \end{array} \right\} \frac{dN_{pT}}{dR} = 1.4 \times 10^{-4} \frac{1}{\mu^+ \text{ cm}} + 6.7 \times 10^{-4} \frac{R}{\mu^+ \text{ cm}^2}.$$

Of course the coefficient of  $R$  in the above expression is only an upper limit since, if an electron scatters before it radiates, any resulting pair will not correlate with the  $\mu^+$  decay.

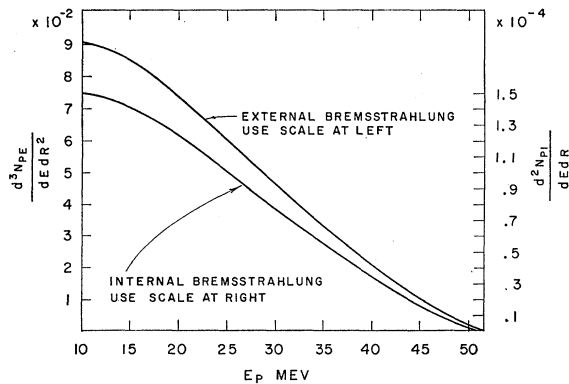


FIG. 7. The spectral distribution of electron pairs from external and internal bremsstrahlung. The function  $d^2 N_{pE}/dE dR^2$  is the differential probability per Mev, per radiation length squared, that an electron from  $\mu$  decay will produce a photon which then creates an electron pair of total energy  $E$  in which both electrons have energy greater than 2 Mev. The function  $d^2 N_{pI}/dE dR$  is the differential probability per radiation length, per Mev, that a photon from  $\mu^+ \rightarrow e^+ + \nu^0 + \bar{\nu}^0 + \gamma$  will produce an electron pair of energy  $E$  in which both electrons have energy greater than 2 Mev.

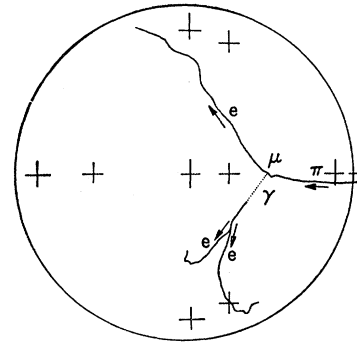
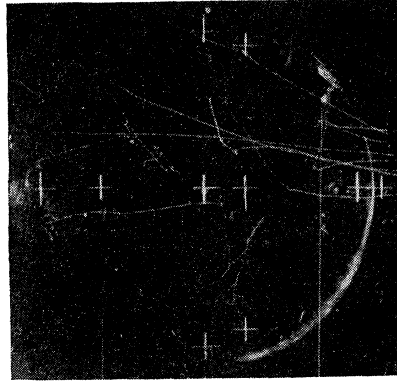


FIG. 8. An example of the decay  $\mu^+ \rightarrow e^+ + \nu^0 + \bar{\nu}^0 + \gamma$ .

A total of  $1.8 \times 10^5$   $\mu^+$  endings were scanned for pairs from  $\mu^+ \rightarrow e^+ + \nu^0 + \bar{\nu}^0 + \gamma$ . The following scanning criteria were used:

- (1) The momentum vector of both the  $\gamma$  ray and the decay electron, when projected on the plane of the front window, made an angle of more than  $30^\circ$  with respect to the front and back beam direction.
- (2) The distance from the  $\mu^+$  ending to the pair vertex was less than 2 cm.
- (3) Both electron and positron in an electron pair had an energy greater than 2 Mev.

Figure 8 shows an example of a possible  $\mu^+ \rightarrow e^+ + \nu^0 + \bar{\nu}^0 + \gamma$  decay.

In Fig. 9 the experimentally determined energy distribution of 313 pairs correlated with  $\mu^+$  decays is plotted. The energy of a pair was determined from range and multiple scattering. Multiple-scattering measurements were made on electrons for which it was possible to obtain at least six second differences and range measurements were made whenever the electron stopped in the illuminated volume of the chamber. When possible, both methods were applied in determining the energy and the results were averaged with equal weights. The curve shown represents the expected spectral distribution. It was obtained by taking the theoretical energy distribution for both internal and external bremsstrahlung and folding into it the energy-dependent detection efficiency. The curve is normalized to 313.

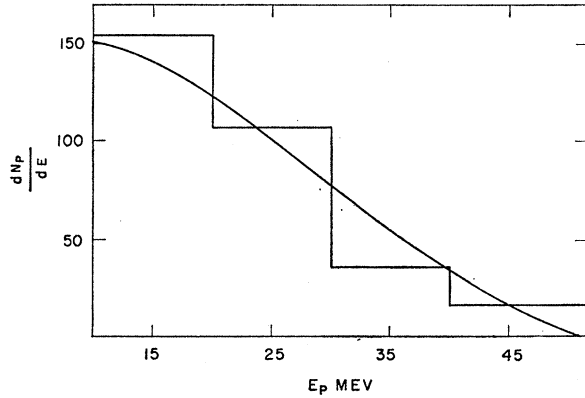


FIG. 9. The experimentally determined energy distribution of 313 electron pairs which were correlated with  $\mu$  decay. The curve through the data is the estimated spectral distribution normalized to 313.

Figure 10 shows the number of correlated pairs with energy greater than 10 Mev plotted as a function of the distance from the  $\mu^+$ -decay point to the pair vertex. The straight line was obtained by applying the maximum likelihood method to the data. A discussion of the maximum likelihood method is given in reference 10.<sup>14</sup> In Fig. 11 the likelihood function is plotted as ordinate and the intercept as abscissa. Figure 12 and Fig. 13 show the results for  $E_0=20$  Mev.

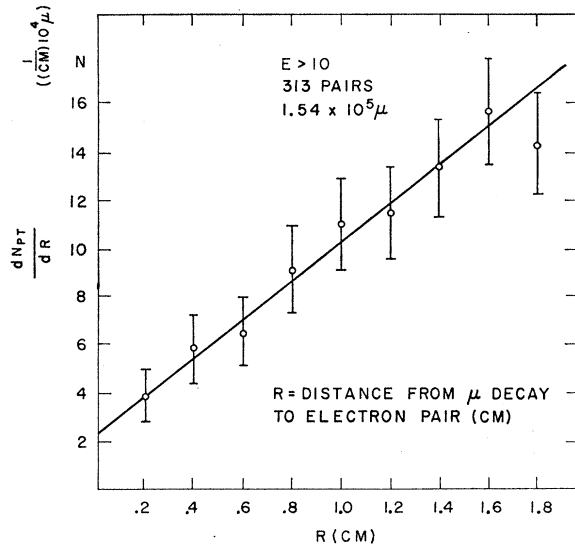


FIG. 10. The spatial distribution  $dN_{pT}/dR$  of 313 electron pairs with energy greater than 10 Mev which were correlated with  $\mu$  decay. The intercept at  $R=0$  is proportional to the branching ratio  $R_I = (\mu^+ \rightarrow e^+ + \nu^0 + \bar{\nu}^0 + \gamma) / (\mu^+ \rightarrow e^+ + \nu^0 + \bar{\nu}^0)$ ,  $E_\gamma > 10$  Mev.

<sup>14</sup> For more general discussions see: M. Annis, W. Cheston, and H. Primakoff, *Revs. Modern Phys.* **25**, 818 (1953); H. Cramer, *Mathematical Methods of Statistics* (Princeton University Press, Princeton, New Jersey, 1946).

The most probable values obtained were

$$\begin{aligned}
 E_0 = 10 \text{ Mev} \left\{ \begin{aligned} \frac{dN_{pT}}{dR} &= 2.3 \times 10^{-4} \frac{1}{\mu^+ \text{ cm}} \\ &+ 7.9 \times 10^{-4} \frac{R}{\mu^+ \text{ cm}^2}, \end{aligned} \right. \\
 E_0 = 20 \text{ Mev} \left\{ \begin{aligned} \frac{dN_{pT}}{dR} &= 0.9 \times 10^{-4} \frac{1}{\mu^+ \text{ cm}} \\ &+ 3.9 \times 10^{-4} \frac{R}{\mu^+ \text{ cm}^2}. \end{aligned} \right.
 \end{aligned}$$

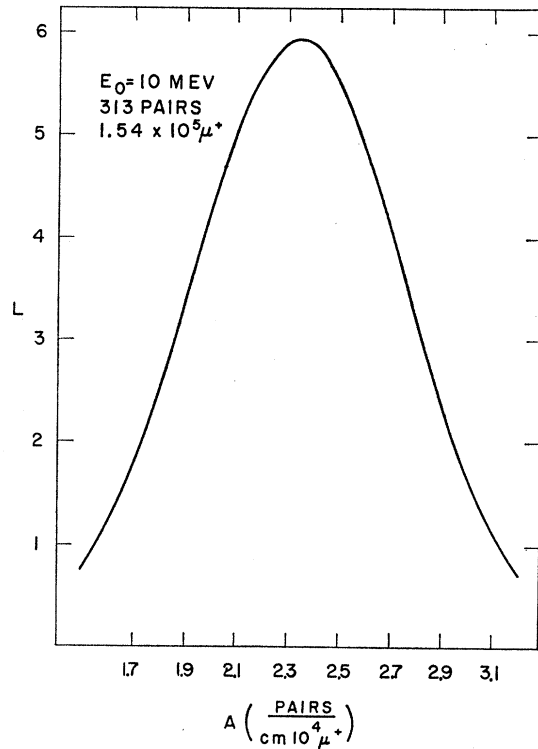


FIG. 11. The likelihood function

$$L = \prod_{i=1}^N (A + Bx_i),$$

for electron pairs with  $E_\gamma > 10$  Mev plotted as a function of  $A$ . The branching ratio  $R_I = (\mu^+ \rightarrow e^+ + \nu^0 + \bar{\nu}^0 + \gamma) / (\mu^+ \rightarrow e^+ + \nu^0 + \bar{\nu}^0)$ ,  $E_\gamma > 10$  Mev, is proportional to  $A$ .

Repeated scanning of several rolls of film indicated that the upper limit on the scanning efficiency was about 85%.

Since the estimated value for the constant term, i.e., the internal bremsstrahlung, was  $2.5 \times 10^{-4}$ , this gives, assuming that the spectral distribution given by Kinoshita and Sirlin is correct,

$$\begin{aligned}
 R_{IB} &= (\mu^+ \rightarrow e^+ + \nu^0 + \bar{\nu}^0 + \gamma) / (\mu^+ \rightarrow e^+ + \nu^0 + \bar{\nu}^0) \\
 &= (1.3 \times 10^{-2})(2.3 \times 10^{-4}) / (2.5 \times 10^{-4})(0.85) \\
 &= (1.4 \pm 0.4) \times 10^{-2}, \quad E_0 = 10 \text{ Mev},
 \end{aligned}$$



and

$$R_{IB} = (4.4 \times 10^{-8})(0.9 \times 10^{-4}) / (1.4 \times 10^{-4})(0.85) \\ = (3.3 \pm 1.3) \times 10^{-3}, \quad E_0 = 20 \text{ Mev.}$$

This is in very good agreement with the theoretical results of Kinoshita and Sirlin, who found

$$R_{IB} = 1.3 \times 10^{-2}, \quad E_0 = 10 \text{ Mev,} \\ R_{IB} = 4.4 \times 10^{-3}, \quad E_0 = 20 \text{ Mev,}$$

The errors were estimated as follows: The accuracy in determining the energy of an electron pair was probably no better than 30%. For  $E_0 = 10$  Mev this introduced an uncertainty about 16% in the detection efficiency and therefore in the branching ratio  $R_{IB}$ . The uncertainty in the intercept of  $dN_{PT}/dR$ , according to the likelihood fit of the data shown in Figs. 10 and 11 introduced an error of 20% in the branching ratio. If these two errors were independent, then the error in  $R_{IB}$  was about 26%. The same procedure was followed for  $E_0 = 20$  Mev and the error in  $R_{IB}(E_0 = 20 \text{ Mev})$  was estimated to be about 40%.

#### D. $\mu^+ \rightarrow e^+ + \nu^0 + \bar{\nu}^0 + e^+ + e^-$

This decay mode would produce three visible electrons whose total energy was between 0 and 106 Mev. In general the momentum of the visible particles would not balance. In fact this process may be looked on as an internal conversion of the  $\gamma$  ray in the process  $\mu^+ \rightarrow e^+ + \nu^0 + \bar{\nu}^0 + \gamma$ . The photon direction in the later process is correlated closely with the electron direction. Therefore, one would expect that in the decay process  $\mu^+ \rightarrow e^+ + \nu^0 + \bar{\nu}^0 + e^+ + e^-$ , the three electrons would tend to come out in the same direction.

Just as in the case of internal bremsstrahlung the branching ratio depends upon the lower limit  $E_0$  of the energy of the detected electrons.

The possible sources of background for this process were the following:

(1) The decay  $\mu^+ \rightarrow e^+ + \nu^0 + \bar{\nu}^0 + \gamma$  where the  $\gamma$  ray was externally converted within 2 mm of the muon vertex. The magnitude of this background was estimated by integrating the experimentally determined spatial distribution of internal and external bremsstrahlung pairs from  $\mu^+$ , as shown in Fig. 10, over the interval  $R=0$  to  $R=1.5$  mm. This gives for  $E_0 = 10$  Mev a background of  $3.5 \times 10^{-6} N_{\mu}$ .

(2) A  $\gamma$  ray entering with the beam or coming from the chamber walls and accidentally producing a pair near a  $\mu^+$  ending. This effect has been estimated in Sec. B of this chapter and was found to be  $6.4 \times 10^{-6} N_{\mu}$ .

The scanning efficiency for this process was taken to be the same as that for internal bremsstrahlung, 85%.

A total of  $3.3 \times 10^5 \mu^+$  decays were scanned for this process. Of these 21 were consistent with

$$\mu^+ \rightarrow e^+ + \nu^0 + \bar{\nu}^0 + e^+ + e^-.$$

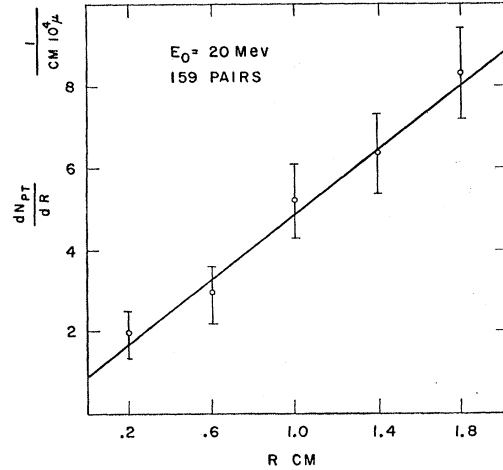


FIG. 12. The spatial distribution of 159 electron pairs having energy greater than 20 Mev which were correlated with  $\mu$  decay. The intercept at  $R=0$  is proportional to the branching ratio  $R_I = (\mu^+ \rightarrow e^+ + \nu^0 + \bar{\nu}^0 + \gamma) / (\mu^+ \rightarrow e^+ + \nu^0 + \bar{\nu}^0)$ ,  $E_\gamma > 20$  Mev.

Thus

$$R_{IC} = (\mu^+ \rightarrow e^+ + \nu^0 + \bar{\nu}^0 + e^+ + e^-) / (\mu^+ \rightarrow e^+ + \nu^0 + \bar{\nu}^0) \\ = [21 - (0.64 + 3.5)(3.3)] / (0.85)(3.3 \times 10^5) \\ = (2.2 \pm 1.5) \times 10^{-5}.$$

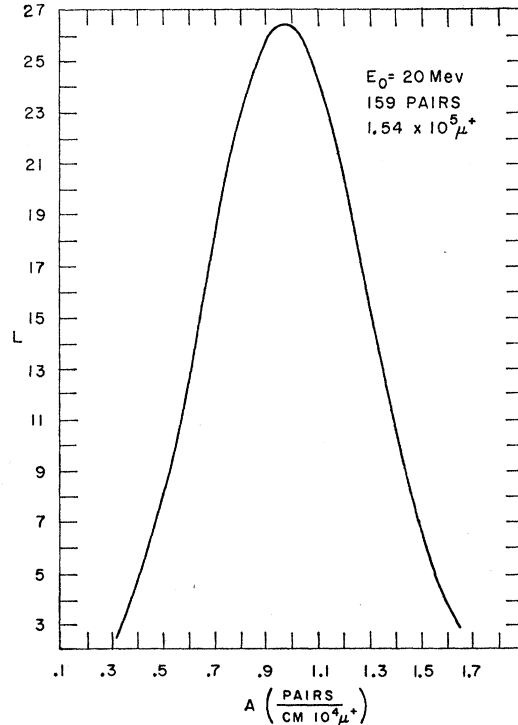


FIG. 13. The likelihood function

$$L = \prod_{i=1}^N (A + Bx_i),$$

for 159 electron pairs which had energy greater than 20 Mev which were associated with  $\mu$  decay. The branching ratio  $R_I = (\mu^+ \rightarrow e^+ + \nu^0 + \bar{\nu}^0 + \gamma) / (\mu^+ \rightarrow e^+ + \nu^0 + \bar{\nu}^0)$ ,  $E_\gamma > 20$  Mev, is proportional to  $A$ .

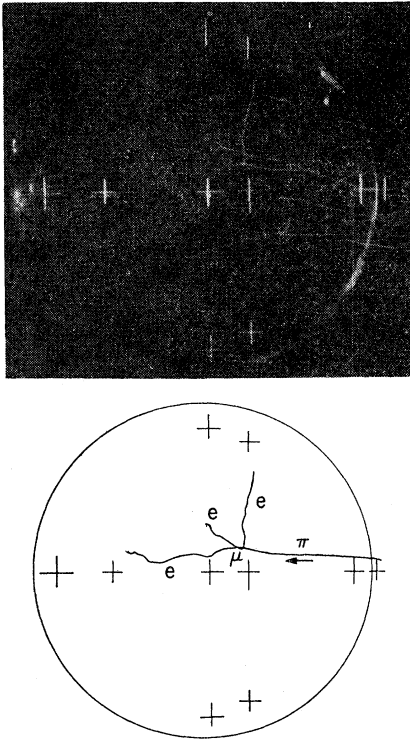


Fig. 14. An example of a  $\mu^+$  decay which can be interpreted as  $\mu^+ \rightarrow e^+ + \nu^0 + \bar{\nu}^0 + e^+ + e^-$ .

Figure 14 shows an example of a  $\mu^+$  decay which can be interpreted to be  $\mu^+ \rightarrow e^+ + \nu^0 + \bar{\nu}^0 + e^+ + e^-$ .

### CONCLUSIONS

Although previous experiments (Table I) using electronic techniques have shown the branching ratio  $R_{\text{rad}} = (\mu^+ \rightarrow e^+ + \gamma) / (\mu^+ \rightarrow e^+ + \nu^0 + \bar{\nu}^0)$  to be less than  $2 \times 10^{-6}$  it is felt that the result of  $R_{\text{rad}}$  less than  $2.5 \times 10^{-5}$  found in this experiment is valuable because of the clearness of visual methods. The results on the internal bremsstrahlung would seem to indicate that the  $\mu^+ \rightarrow e^+ + \gamma$  mode could easily have been detected by this experiment, if the rate were as high as a few times  $10^{-4}$  as predicted by several intermediate-particle theories.

As a result of the low branching ratios for  $\mu^+ \rightarrow e^+ + \gamma$  and  $\mu^+ \rightarrow e^+ + e^- + e^+$ , one of the following conclusions seems to be indicated:

(1) Lepton conservation holds with  $e^-$  and  $\mu^-$  having the same lepton number and both of these leptons are coupled to a neutrino having the same chirality. The absence of  $\mu^+ \rightarrow e^+ + e^- + e^+$  then indicates that the  $\mu$  decays through a charged intermediate boson and the absence of  $\mu^+ \rightarrow e^+ + \gamma$  indicates that

- (a) The boson is not scalar.
- (b) The boson, if vector, is either very massive or has an anomalous magnetic moment near 0.7.

(2) The muon decays through an intermediate boson either vector or scalar and lepton conservation holds, but  $e^-$  and  $\mu^-$  have opposite lepton numbers and are coupled to neutrinos of opposite chiralities.

(3) The muon decay is direct, but the coupling to three electrons is small.

If the second of these theories is correct, then the decay mode  $\mu^+ \rightarrow e^+ + \nu^0 + \bar{\nu}^0 + \gamma$  would be a possible means of detecting the intermediate boson. The effect on this branching ratio of a charged intermediate boson with mass near that of the  $K$  meson has been estimated to be a few percent. Unfortunately the experiment reported in this paper was not sensitive enough to detect such an effect. The primary difficulties in such an experiment are the measurement of  $\gamma$ -ray energies and discrimination against the high background of  $\gamma$  rays from external bremsstrahlung.

If the muon decay is a direct interaction, then the limit on the branching ratio for 3-electron decay can be used to estimate the upper limit on the coupling of the  $\mu$  to three electrons. Since the electron mass is small compared to that of the muon, the phase space available in three-electron decay is approximately the same as in the normal decay into an electron and two neutrinos. One would expect the matrix element to be the same also. Thus the couplings should be related by

$$g'^2/g^2 = R_{3e} = (\mu^+ \rightarrow e^+ + e^- + e^+) / (\mu^+ \rightarrow e^+ + \nu^0 + \bar{\nu}^0),$$

where  $g$  is the weak interaction coupling constant and  $g'$  is a measure of the coupling of the  $\mu$  to three electrons. If we total all of the results on the measurement of  $\mu^+ \rightarrow e^+ + e^- + e^+$ , including those reported in this paper and those found by other experimenters as tabulated in Table II we find

$$g' < 1.2 \times 10^{-3} g.$$

### ACKNOWLEDGMENTS

We wish to thank R. Sutton and the engineering staff at the Carnegie Institute of Technology synchrocyclotron for making the laboratory facilities available and for their assistance in this experiment. In particular we wish to thank S. De Benedetti, T. Fields, I. Nadelhaft, T. Romanowski, G. Pewitt, and R. Siegel for assistance in various phases of the experiment.

We would like to thank J. Scandrett and R. Willmann from the University of Wisconsin and J. Parker from Michigan State University for being of such great assistance in making the exposure.

The scanning was done very efficiently by Mr. and Mrs. F. Chen, Mrs. L. Eggman, and L. Lee.

We wish to thank P. Schultz and A. Swenson for their part in constructing the bubble chamber used in this experiment.

E. Albright and the staff of the University of Wisconsin Numerical Analysis Laboratory provided generous assistance in the use of the IBM 650.

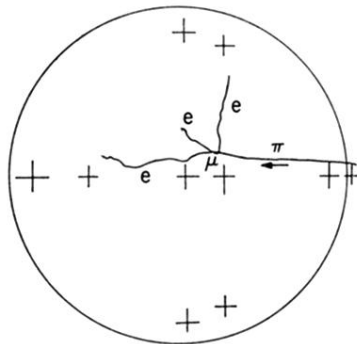
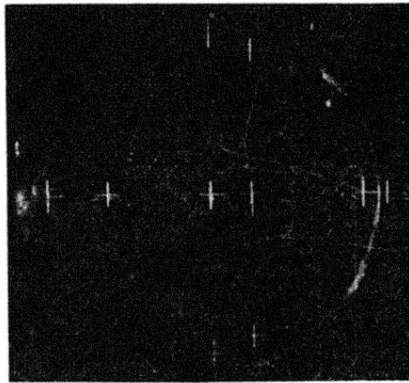


FIG. 14. An example of a  $\mu^+$  decay which can be interpreted as  $\mu^+ \rightarrow e^+ + \nu^0 + \bar{\nu}^0 + e^+ + e^-$ .

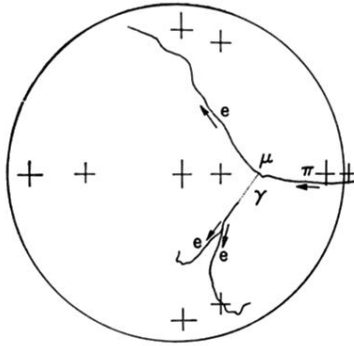
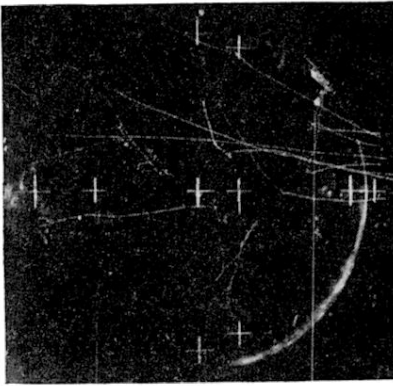


FIG. 8. An example of the decay  $\mu^+ \rightarrow e^+ + \nu^0 + \bar{\nu}^0 + \gamma$ .